Journal of Inflammation Research

Dovepress
Taylor & Francis Group

Open Access Full Text Article

ORIGINAL RESEARCH

Lactate Ameliorates Kainic Acid-Induced Neuroinflammation and Cognitive Impairment via the Chemokine Signaling Pathway in Mice

Xiaoqi Chu[1,2,*], Yusong Ge[3,*], Chao Geng[1,2], Peipei Cao[1,2], Penghu Wei[2], Bin Fu[2], Zihao Deng[4], Yuhao Li[5,6], Guoguang Zhao[2,7]

[1]Optometry Institute, School of Medicine Nankai University, Tianjin, People's Republic of China; [2]Department of Neurosurgery, Xuanwu Hospital Capital Medical University, Beijing Municipal Geriatric Medical Research Center, Beijing, People's Republic of China; [3]Department of Neurology, The Second Hospital of Dalian Medical University, Dalian, People's Republic of China; [4]Cancer Center, Capital Medical University, Beijing, People's Republic of China; [5]Central Laboratory, Xuanwu Hospital Capital Medical University, Beijing Municipal Geriatric Medical Research Center, Beijing, People's Republic of China; [6]Department of Pathology, School of Medicine Nankai University, Tianjin, People's Republic of China; [7]National Medical Center for Neurological Diseases, Beijing, People's Republic of China

*These authors contributed equally to this work

Correspondence: Guoguang Zhao, Department of Neurosurgery, Xuanwu Hospital Capital Medical University, Beijing Municipal Geriatric Medical Research Center, Beijing, People's Republic of China, Email ggzhao@vip.sina.com; Yuhao Li, Central Laboratory, Xuanwu Hospital Capital Medical University, Beijing Municipal Geriatric Medical Research Center, Beijing, People's Republic of China, Email liyuhao@xwhosp.org

Purpose: Lactate, previously considered a metabolic waste product, has been shown to have neuroprotective potential. This study aims to investigate the impact of lactate intervention and its underlying mechanisms on epilepsy.

Methods: HT22 cells were stimulated with glutamate to construct an excitotoxicity cell model. An acute epilepsy model was established in mice by kainic acid induction. The neuronal damage, microglial activation, inflammatory responses, and functional changes were determined by TUNEL assays, immunohistochemistry, quantitative real-time polymerase chain reaction and behavioral tests. The differentially gene expression and functional enrichment were analyzed with RNA sequencing.

Results: The in vitro lactate intervention reduced the number of apoptotic cells, the release of inflammatory factors, and the expression of vesicular glutamate transporter 1. In mice with acute epilepsy, lactate treatment mitigated neuronal damage, microglial activation, and inflammatory responses in the hippocampus and ameliorated anxiety-like behavior and cognitive impairment.

Conclusion: Lactate exerts therapeutic effects on epilepsy through the chemokine signaling pathway. The neuroinflammation is an important contributor to cognitive impairment. Targeting inflammatory pathways is a promising strategy for improving the prognosis of epilepsy.

Keywords: lactate, neuroinflammation, cognitive impairment, neuronal damage, chemokine, epilepsy

Introduction

Epilepsy is one of the most common brain disorders, affecting more than 70 million people worldwide. It is characterized by spontaneous recurrent seizures and manifests as sensory, motor, autonomic, psychiatric, memory, and behavioral abnormalities. To date, the pathogenesis of epilepsy has not been fully elucidated. For most patients, antiepileptic drugs are the first-line treatment used to control seizures.[1] However, more than half of patients taking antiepileptic drugs still have seizures, which poses a major burden and challenge for patients, caregivers, families, and society.[2] Seizures cause abnormal glial activation, increased proinflammatory factor levels, and elevated chemokine levels, ultimately leading to irreversible neuron loss, and neurological dysfunction.[3,4] Therefore, there is an urgent need to develop new therapeutic approaches to suppress neuroinflammation and mitigate neuronal damage caused by epileptic seizures.

Lactate, previously considered a metabolic waste product, has recently been found to influence multiple biological processes by acting as a substrate for metabolic processes or as a signaling molecule. Lactate and ATP are produced by glycolysis under hypoxic or aerobic conditions. Then lactate is subsequently transported to other cells by monocarboxylate

Received: 30 September 2024
Accepted: 20 January 2025
Published: 27 January 2025

Graphical Abstract

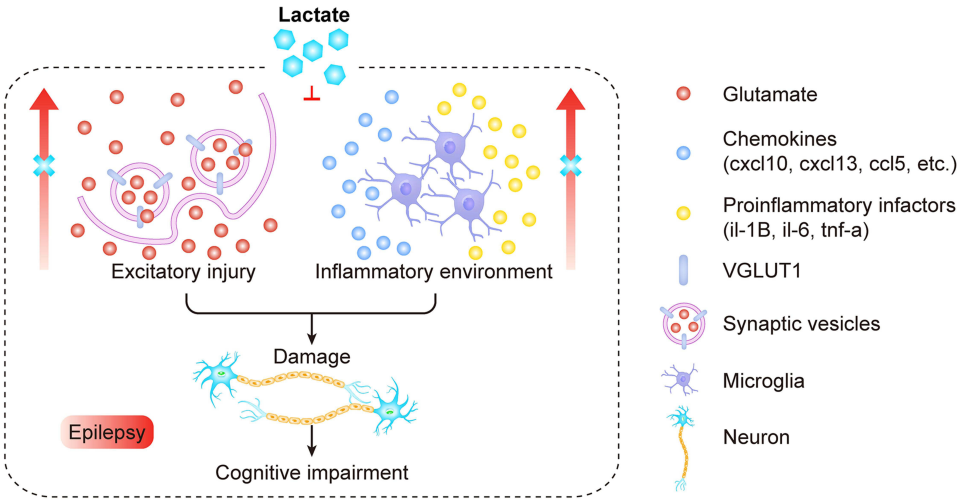

transporters to participate in and regulate energy metabolism.[5] Hydroxy-carboxylic acid receptor (HCAR), a member of the G protein-coupled receptor family, has three subtypes, namely, HCAR1, HCAR2 and HCAR3. Lactate can act as an endogenous ligand and a signaling molecule by specifically activating HCAR1. It has been reported that the lactate/HCAR1 system is involved in pathophysiological processes of the cardiovascular system, digestive system, and neoplastic diseases.[6–8] Moreover, in the central nervous system, HCAR1 is highly expressed in the cerebral cortex, hippocampus, and astrocytes.[9] Recently, lactate intervention has attracted increasing attention from researchers due to its ability to promote neurogenesis and synaptic plasticity and alleviate neurotoxicity.[10–12] However, little is known about the impact of lactate intervention on epilepsy.

In recent years, the rapid development of omics technology has provided a new perspective for biomedical research.[13,14] It can be used to identify biomarkers for disease diagnosis and to improve the understanding of disease pathogenesis in order to propose novel targeted therapies. Common omics technologies include genomics, transcriptomics, proteomics, and metabolomics.[15–17] Genomics detects alterations in the genetic information of an organism at the DNA level. Transcriptomics studies the transcriptional expression of all genes in a specific state and focuses on changes at the RNA level. Proteomics and metabolomics are important in exploring the role of biomolecules by analyzing the expressed proteins and small molecule metabolites in a sample qualitatively and quantitatively. Among these, transcriptomics offers a dynamic perspective and a more intuitive understanding of gene regulation patterns.

In this study, neuronal apoptosis and glutamate transport were first examined in a lactic acid-treated in vitro excitotoxic injury model. Second, inflammatory responses, neuronal damage, and functional changes following lactate treatment were evaluated in an acute epilepsy mouse model. Finally, the gene expression profiles, gene functions, and the underlying mechanisms of lactate intervention were explored by RNA sequencing (RNA-seq). Our study might help to broaden our view of the potential of the lactate/HCAR1 system as a target in epilepsy therapy.

Material and Methods

Cell Line and Animal

The mouse hippocampal-derived cell line HT22 was obtained from American Type Culture Collection (ATCC; Manassas, VA, USA). The cells were cultured in high-glucose Dulbecco's modified Eagle's medium (DMEM; Gibco BRL, Gaithersburg, MD, USA) supplemented with 10% fetal bovine serum (FBS; Gibco BRL) and 1% penicillin–streptomycin (Gibco BRL) in an incubator supplied with 5% CO_2 at 37 °C. Specific pathogen-free (SPF) male C57BL/6 mice (eight weeks old, 20–25 g) were purchased from Charles River Laboratory Animal Technology Co., Ltd. (Beijing, China). All mice were housed in cages at

a temperature of 23±2 °C with a relative humidity of 40–70% under a 12-h light/12-h dark cycle and given access to food and water *ab libitum*. All animal experiments were approved by the Laboratory Animal Welfare and Ethics Committee of Xuanwu Hospital Capital Medical University (permission number: XW20220906-1) and were performed in compliance with the National Institutes of Health Guide for the Care and Use of Laboratory Animals.

Cell Excitotoxicity Induction and Lactate Treatment

HT22 cells were seeded into 96-well plates at a density of 8×10^3 cells/well and stimulated with L-glutamic acid (glutamate; MedChemExpress LLC., Shanghai, China) at concentrations of 0 (control), 5, 10, 15, 20, and 25 mM for 24 h. A cell counting kit-8 (CCK-8; Solarbio, Beijing, China) was used to assess cell viability and determine the concentrations for glutamate stimulation and L-(+)-lactic acid (lactate, L1750; Sigma–Aldrich, St. Louis, MO, USA) treatment. HT22 cells were then seeded into 6-well or 24-well plates and divided into three groups. In the glu group, cells were cultured with the serum-free culture medium containing glutamate at a concentration of 20 mM to induce cell excitotoxicity; in the lactate group, cells were cultured with the serum-free culture medium containing glutamate at a concentration of 20 mM and lactic acid at a concentration of 1 mM. Cells cultured in serum-free medium without any stimulation or treatment were used as the control group.

TUNEL Assay

A one-step TUNEL apoptosis assay kit (Beyotime, Shanghai, China) was used to detect HT22 cell death according to the manufacturer's instructions. The cell slides were mounted with the anti-fade mounting medium supplemented with DAPI and photographed using a Nikon ECLPSE TI confocal microscope (Japan) at excitation wavelengths of 594 nm and 405 nm.

Acute Seizure Model and Epilepsy Treatment

To induce acute seizures, the mice were given a single intraperitoneal injection of kainic acid (KA; Abcam, Cambridge, MA, USA) at a dose of 30 mg/kg. Mice were observed within 1 h after KA induction. The seizure severity was evaluated according to the Racine scale: grade 0, normal behavior with controlled breathing; grade 1, immobility or freezing, facial twitching, and chewing with fast breathing; grade 2, head bobbing and facial jerks; grade 3, repeated head nodding or forelimb clonus; grade 4, forelimb clonus and rearing with possible falling; grade 5, generalized tonic-clonic activity with loss of postural tone; and grade 6, status epilepticus (SE) or death.[18] To standardize the measurement of acute seizures, mice that experienced more than two consecutive grade 4 or higher seizures were considered successfully modeled. Mice were randomly divided into three groups: mice with KA induction were used as the KA group; mice treated with sodium L-lactate (L7022; Sigma–Aldrich) at a dose of 2g/Kg by daily intraperitoneal injection for 5 days after KA induction were used as the lactate group; and mice injected with an equal volume of 0.9% saline were used as the control group.

Behavioral Tests

All behavioral tests were performed at 5 days post-KA induction in a soundproof, quiet, and dim testing room between 09:30 and 16:30 to avoid the potential influence of circadian rhythms. Before any tests were performed, the mice were left in the testing room for 1 h to acclimate to the environment. For the open field test, the mice were placed in the center of a white cube opaque plastic box (50 cm×50 cm×50 cm) and allowed to roam freely for 5 min. A camera was used to monitor and record the locomotor activity of the mice. The time spent in the center, the distance traveled in the center, and the total distance travelled were analyzed by Noldus EthoVision XT17 software (Noldus Information Technology, Wageningen, Netherlands).

For the rotarod test, the mice were placed on the rotarod (KEW, Nanjing, China) at a starting speed of 4 rpm for 30s, then on the rotarod accelerated from 0 to 40 rpm for 5 min, and finally rotated at 40 rpm for another 1 min. This test was performed three times for each animal, and the average time spent on the rotarod and distance traveled on the rotarod were recorded and analyzed.

The novel object recognition test was carried out in a white cube opaque plastic box (50 cm×50 cm×50 cm). Two objects with the same color, shape, and size were placed in the box. Mice were placed in the center of the box and

subjected to 10 min of training. One hour later, one object was replaced by a novel object with a different shape and color, and each mouse was returned to the box for a 10-min test. The routes of mice and the time spent sniffing novel and familiar objects were recorded and calculated using Noldus EthoVision XT17 software (Noldus). The discrimination index was calculated as follows to evaluate short-term memory.

$$\text{Discrimination index} = \frac{\text{time (spent exploring novel object)}}{\text{time (spent exploring novel and familiar objects)}}$$

Brain Tissue Collection and Preparation

Upon completion of the behavioral tests, the mice were deeply anesthetized with sodium pentobarbital (50 mg/kg) via intraperitoneal injection. Transcardial perfusion was carried out with 0.9% saline and 4% paraformaldehyde at 4 °C. The brains were dissected, fixed in 4% paraformaldehyde for 24 h at 4 °C, cryoprotected in 30% sucrose in 0.1 M phosphate-buffered saline (PBS, pH 7.4) for 24 h, and frozen in optimal cutting temperature compound (OCT; Sakura Finetek, CA, USA). Coronal sectioning at a thickness of 10 μm was performed using a cryostat microtome (Leica, Wetzlar, Germany). For quantitative real-time polymerase chain reaction (qRT–PCR) assays, the hippocampi were dissected immediately after transcardial perfusion. All cryosections and tissue samples were stored at −80 °C until use.

Immunofluorescence and Immunohistochemistry

Immunofluorescence and immunohistochemistry were performed using standard procedures. Briefly, HT22 cells from the three groups were seeded into 24-well plates at a density of 3×10^4 cells/well, fixed with 4% paraformaldehyde for 15 min, and permeabilized with 0.1 M PBS and 0.5% Triton X-100 (PBST) for 20 min at room temperature. For immunohistochemistry, cryosections were washed three times with 0.1 M PBS for 5 min and permeabilized with 0.5% PBST for 30 min. The primary antibodies used were anti-NeuN (1:500; ab177487, Abcam), anti-Iba1 (1:500; ab48004, Abcam) and anti-VGLUT1 (1:500; SYS-135304, Synaptic Systems, Goettingen, Germany) antibodies. The secondary antibodies used were Alexa Fluor 488 (1:1000; Thermo Fisher Scientific, Waltham, MA, USA) and Alexa Fluor 594 (1:1000; Thermo Fisher Scientific). 4',6-Diamidino-2-phenylindole (DAPI; Sigma–Aldrich) was used to label the nuclei. Images of the immunostained sections were obtained using a Nikon ECLPSE TI confocal microscope.

Western Blot Analysis

Total protein was extracted from hippocampal tissues using lysis buffer (CWBIO, Beijing, China). The concentration was calculated according to the BCA protein quantitative assay kit (CWBIO). The anti-NeuN antibody (1:500) was used as the primary antibody in this study. Anti-β-actin (1:20000; Proteintech, Chicago, IL, USA) was used as a loading control. The secondary antibodies were anti-horseradish peroxidase (HRP)-rabbit (1:5000; Abcam) antibody and anti-horseradish peroxidase (HRP)-mouse (1:5000; Proteintech). Optical density analysis was performed using ImageJ software (ver. 1.8.0, National Institute of Health (NIH), Bethesda, MD, USA, http://rsb.info.nih.gov/ij/), and the data were normalized to the internal standard β-actin.

qRT–PCR

Total RNA was extracted from HT22 cells or mouse hippocampi using a FastPure Cell/Tissue Total RNA Isolation Kit (Vazyme, Nanjing, China). Hifair® III 1st Strand cDNA Synthesis SuperMix (Yeasen, Shanghai, China) was used for reverse transcription, and Hieff® qPCR SYBR Green Master Mix (Yeasen) and a LightCycler 480 II (Roche, Switzerland) were used for qRT–PCR. The protocol was as follows: 5 min at 95 °C followed by 40 cycles of 10 s at 95 °C, 20 s at 60 °C, and 20 s at 72 °C. The relative expression levels of mRNA were analyzed using the $2^{-\Delta\Delta Ct}$ method and normalized to those of β-actin. The primer sequences used are listed in Table 1.

Table 1 Primer Sequences for qRT-PCR

Gene	Primer	Sequence (5'-3')
β-actin	Forward	CTACCTCATGAAGATCCTGACC
	Reverse	CACAGCTTCTCTTTGATGTCAC
c-fos	Forward	GAATCCGAAGGGAACGGAATAA
	Reverse	GCAACGCAGACTTCTCATCT
hcar1	Forward	CTCCTCTACTCATCCTGGTCTT
	Reverse	GTGCTTGACTTCCAGGTCTT
vglut1	Forward	TACTGGAGAAGCGGCAGGAAGG
	Reverse	GATGGCGATGATGTAGCGACGAG
il-1β	Forward	AAAGCTCTCCACCTCAATGG
	Reverse	CCCAAGGCCACAGGTATTT
il-6	Forward	CTTCCATCCAGTTGCCTTCT
	Reverse	CTCCGACTTGTGAAGTGGTATAG
tnf-α	Forward	TGTCTACTCCCAGGTTCTCTT
	Reverse	GCAGAGAGGAGGTTGACTTTC
fcnb	Forward	GCTTGACGGCTCTGTGGACTTC
	Reverse	TCACTGGTTCCCTGGGTGGTTAG
trdn	Forward	GCCAAAGAAACTCCGAAAACACCAC
	Reverse	CTCCTGCTGTCTCCTCCTCCTG
fam124b	Forward	CCCAATCCGTGTGTTCCCATCAG
	Reverse	CACCTCTCAAGCAGCCGTTCAAG
olfr5	Forward	GTGGCTATTGGCAGGGCAGTTC
	Reverse	GGCGGGCATAGATGAAGATAGTGAC
emilin3	Forward	GCTGCTGTCTGAGAATGGAGGTG
	Reverse	GCTGATCTGTCTGGTATGGCACTC
lrr1	Forward	TGCCCGAGTTGATATGCGTATGC
	Reverse	TCTTGAAGGTGGGTGAGGTCTCC
slc15a1	Forward	CCTCACAGACCACGACCACAATG
	Reverse	ATCGCCACCAAACGCAGACAC
gbp10	Forward	GGCCTTCATCGAGAGTTCCATCTTG
	Reverse	GCTGCTCCTTCTGCTTCTGTCTTAG

RNA-Seq and Bioinformatics Analysis

Total RNA from the hippocampi of mice in the control, KA, and lactate groups was used for RNA-seq. The RNA concentration and purity were assessed using a Nanodrop spectrophotometer (Thermo Fisher Scientific). Total RNA (0.4 μg) from each sample was used for library preparation. RNA sequencing was performed using a 2×150 bp paired-end configuration on an Illumina NovaSeq 6000 instrument (Illumina, San Diego, CA, USA) by Novogene Co., Ltd. (Beijing, China). The data were generated from five biological replicates in each group.

The DESeq2 package (v1.20.0) in R software was used to perform the differential expression analysis, which used a model based on negative binomial distribution. Differences with a P value < 0.05 and $\log_2$ fold change ≥ 1 were considered significant. The "ClusterProfiler" R package (v3.8.1) was used to carry out Gene Ontology (GO) and Kyoto Encyclopedia of Genes and Genomes (KEGG) enrichment analysis in R, and Gene Set Enrichment Analysis (GSEA) was performed using the "GSEA" package (v3.0) in R. The STRING online tool (https://cn.string-db.org/) was used to construct protein–protein interaction (PPI) networks, which were then visualized with Cytoscape software (v3.10.1). Weighted Gene Co-expression Network Analysis (WGCNA) was performed on the transcriptome data using the "WGCNA" package (v1.69) in R. Correlations were evaluated using Pearson correlation analysis.

https://doi.org/10.2147/JIR.S498738

Statistical Analysis

ImageJ software (ver.1.8.0, NIH) was used to quantitate and analyze the positively-stained areas and determine the fluorescence intensities of TUNEL, VGLUT1, NeuN, and Iba1. Statistical analysis was carried out with Prism 8.0 software (GraphPad Software, La Jolla, CA, USA). Data were presented as the mean ± standard deviation (SD). Differences among three or more groups were compared using one-way analysis of variance (ANOVA), followed by Tukey's post hoc test. A P value < 0.05 was considered to indicate statistical significance.

Results

Lactate Treatment Reduces Apoptosis and Activates HCAR1 Expression in HT22 Cells

In this study, mouse hippocampal-derived HT22 cells were stimulated with glutamate to establish an in vitro excitotoxic injury model. The CCK-8 assay results showed that glutamate at concentrations of 15 mM or higher significantly decreased cell viability, and HT22 cell viability was less than 80% after glutamate treatment at 20 mM and above (Figure 1A; ANOVA, $^{**}P < 0.01$, $^{****}P < 0.0001$). Hence, 20 mM was selected as the concentration for inducing excitotoxicity. The cytotoxicity of lactate to HT22 cells was also evaluated by a CCK-8 assay. No significant difference was found at concentrations ranging from 1 to 10 mM, and 1 mM was chosen as the safe concentration for further experiments (Supplemental Figure 1; ANOVA, $^{****}P < 0.0001$). In addition, the qRT–PCR analysis revealed that the expression of *c-fos*, an immediate-early gene and a marker of neuronal activity, was dramatically upregulated in glutamate-stimulated HT22 cells and substantially downregulated following lactate treatment (Figure 1B; ANOVA, $^{**}P < 0.01$, $^{****}P < 0.0001$). TUNEL staining revealed that the number of apoptotic cells increased significantly in the glu group; however, the number of apoptotic cells in the lactate group was much lower than that in the glu group (Figure 1C and D; ANOVA, $^{***}P < 0.001$, $^{****}P < 0.0001$). Moreover, lactate treatment significantly increased the expression of *hcar1* in HT22 cells (Figure 1E; ANOVA, $^{***}P < 0.001$). The above data suggest that in vitro lactate treatment reduces neural activity and apoptosis and activates the expression of *hcar1*.

Lactate Treatment Inhibits the Upregulation of VGLUT1 and Inflammatory Responses Induced by Glutamate

The transport of glutamate was detected by labeling vesicular glutamate transporter 1 (VGLUT1) using an immunofluorescent tag. Few VGLUT1-positive signals were detected in the control group. After glutamate stimulation, many bright fluorescent signals were located in the nuclei and cytoplasm of HT22 cells, indicating an increase in glutamate transport during excitotoxic injury (Figure 2A). However, following lactate treatment, the VGLUT1/DAPI area ratio and the VGLUT1/DAPI fluorescence intensity ratio were significantly decreased (Figure 2A–C; ANOVA, $^{*}P < 0.05$, $^{***}P < 0.001$, $^{****}P < 0.0001$). The mRNA expression of vglut1 showed a similar trend among the three groups (Figure 2D; ANOVA, $^{*}P < 0.05$, $^{**}P < 0.01$). Moreover, the expression levels of the inflammatory factors *il-1β, tnf-α* and *il-6* were notably increased in the glu group but markedly decreased in the lactate group (Figure 2E–G; ANOVA, $^{*}P < 0.05$, $^{**}P < 0.01$, $^{****}P < 0.0001$). These data reveal that lactate treatment reduces the transport of glutamate and alleviates cellular inflammatory responses.

Lactate Treatment Attenuates Neuronal Injury in the Hippocampi of Mice With Acute Epilepsy

The in vivo experiments were summarized in Figure 3A. A mouse model of acute epilepsy was established by intraperitoneal administration of KA. NeuN immunohistochemistry was performed to specifically label the surviving hippocampal neurons. Compared to that in the control group, the NeuN/DAPI ratio in the cornu ammonis 1 (CA1) region decreased sharply in the KA group; however, the ratio increased significantly following lactate treatment (Figure 3B and C; ANOVA, $^{*}P < 0.05$, $^{**}P < 0.01$). Moreover, there was no significant difference between the control and lactate groups (Figure 3B and C; ANOVA). The immunostaining for NeuN in the dentate gyrus (DG) region showed a similar trend (Figure 3C and D; ANOVA, $^{*}P < 0.05$, $^{**}P < 0.01$). Western blot analysis revealed that the expression level of NeuN was elevated significantly following the lactate treatment (Figure 3E and F; ANOVA, $^{**}P < 0.01$). The above data not

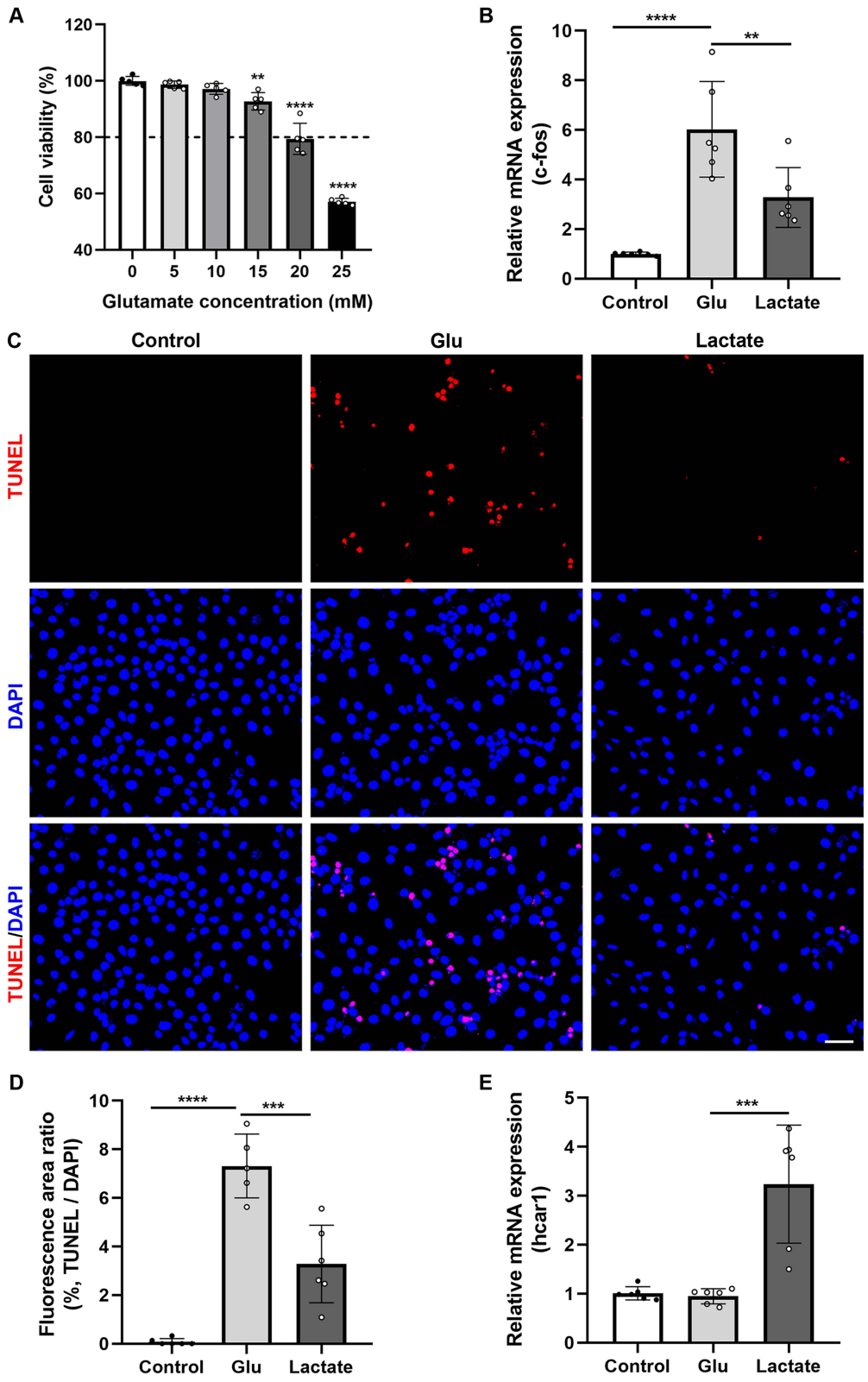

Figure 1 The expression of *c-fos, hcar1* and apoptosis in HT22 cells following glutamate stimulation and lactate treatment. (**A**) Viability of HT22 cells treated with glutamate at different concentrations (0, 5, 10, 15, 20 and 25 mM) for 24 h (n=5 at each concentration). (**B**) The relative mRNA expression levels of *c-fos* in the control, glu and lactate groups (n=6 in each group). (**C**) Fluorescence images of TUNEL staining of HT22 cells in the control, glu and lactate groups. Scale bar: 50 μm. (**D**) Statistical analysis of the ratio of the TUNEL-positive area (n=6 in the control and lactate groups, n=5 in the glu group). (**E**) The relative mRNA expression level of hcar1 (n=6 in each group). The data are presented as the means ± SDs. Significance was determined by one-way ANOVA followed by Tukey's post hoc test (***P*<0.01, ****P*<0.001, *****P*<0.0001).

https://doi.org/10.2147/JIR.S498738

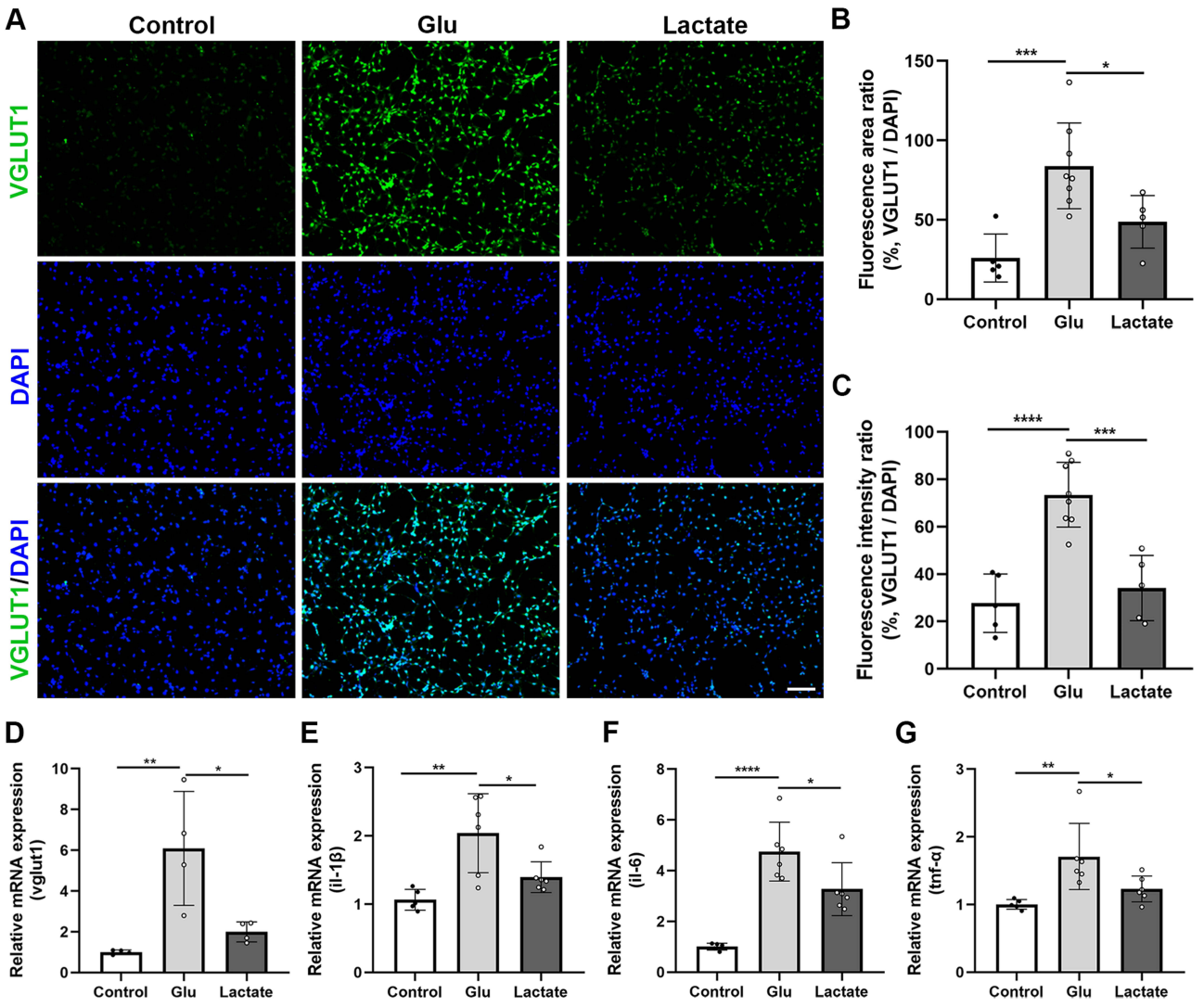

Figure 2 The expression of VGLUT1 and inflammatory factors in HT22 cells following glutamate stimulation and lactate treatment. (**A**) Images of VGLUT1 fluorescence staining in HT22 cells from the control, glu and lactate groups. Scale bar: 100 μm. (**B** and **C**) Quantification of the ratio of VGLUT1/DAPI area (**B**) and the ratio of VGLUT1/DAPI intensity (**C**) (n=5 in the control and lactate groups, n=8 in the glu group). (**D**) The relative mRNA expression levels of vglut1 in the control, glu and lactate groups (n=4 in each group). (**E**–**G**) The relative mRNA expression levels of the inflammatory factors *il-1β* (**E**), *il-6* (**F**) and *tnf-α* (**G**) in HT22 cells (n=5 in the control group, n=6 in the glu and lactate groups). The data are presented as the means ± SDs. Significance was determined by one-way ANOVA followed by Tukey's post hoc test (**P*<0.05, ***P*<0.01, ****P*<0.001, *****P*<0.0001).

only indicate that KA induction leads to obvious cell death in the hippocampi of acute epileptic mice but also demonstrate that lactate treatment effectively reduces neuronal loss.

Lactate Treatment Inhibits Microglial Activation and Neuroinflammation

qRT–PCR analysis revealed that the expression levels of the inflammatory factors *il-1β, il-6*, and *tnf-α* in the hippocampus were increased after KA induction; however, they decreased markedly after lactate treatment (Figure 4A–C; ANOVA, **P* < 0.05, ***P* < 0.01, ****P* < 0.001, *****P* < 0.0001). The Iba1 antibody was used as a specific marker of microglia. In the control group, almost no fluorescent signal was detected. In the KA group, Iba1-positive cells were increased in the CA1 region, indicating that the microglia were strongly activated under epileptic conditions. In contrast, few Iba1-expressing cells were detected in the lactate group (Figure 4D and E; ANOVA, ***P* < 0.01, ****P* < 0.001). A similar trend was observed for the immunostaining of NeuN in the DG region (Figure 4F and G; ANOVA, ***P* < 0.01, ****P* < 0.001). The above data illustrate that lactate treatment is capable of suppressing the release of inflammatory factors and the activation of microglia.

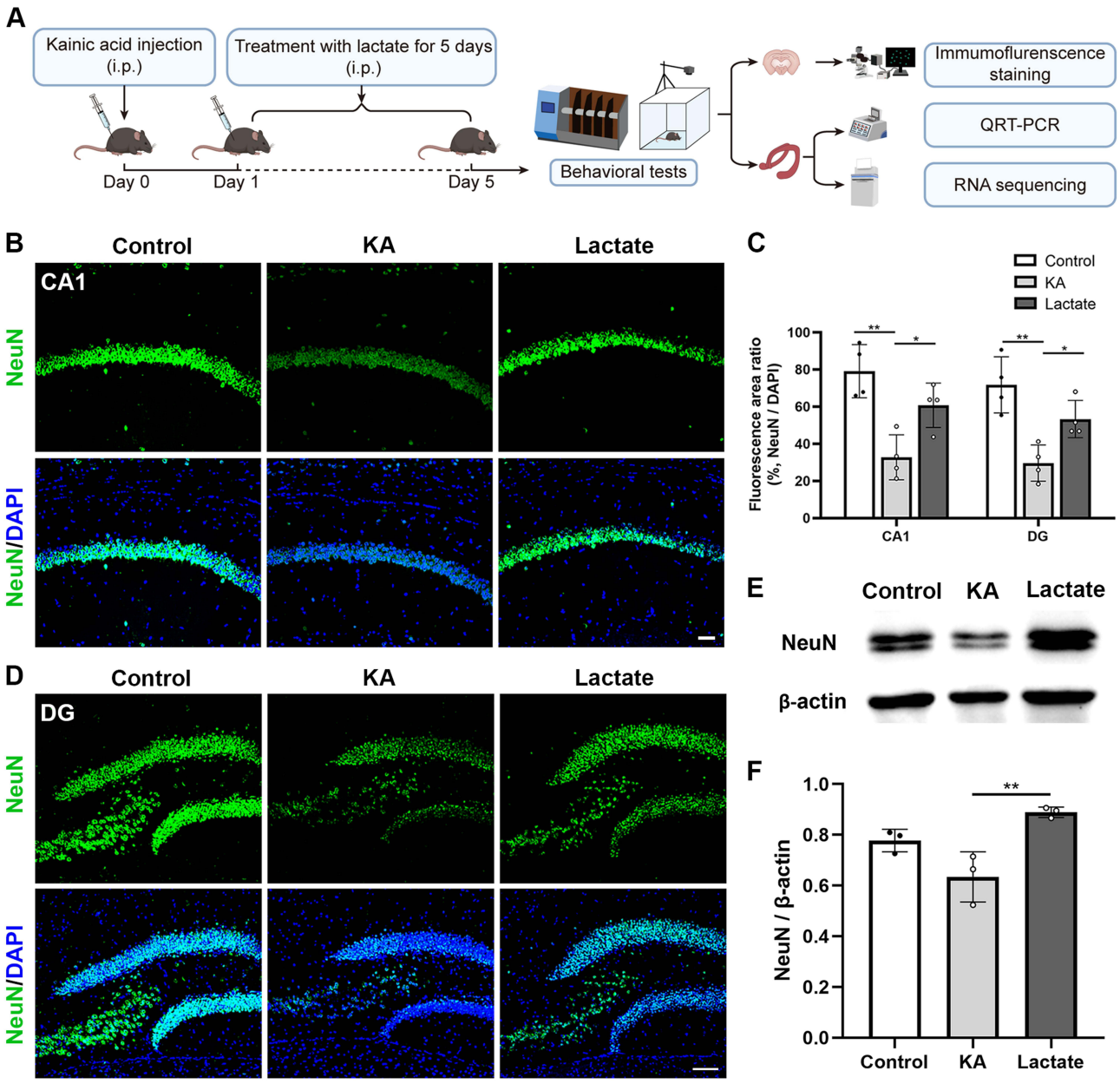

Figure 3 Neuronal damage in the hippocampi of acute epileptic and lactate-treated mice. (**A**) Schematic diagram of the animal experiments. (**B**) Immunofluorescence images of NeuN in the cornu ammonis 1 (CA1) region of the hippocampus in the control, KA and lactate groups. Scale bar: 50 μm. (**C**) Statistical analysis of the NeuN/DAPI area ratio in the CA1 and dentate gyrus (DG) regions (n=4 in each group). (**D**) Immunofluorescence images of NeuN in the DG region of the hippocampus in the control, KA and lactate groups. Scale bar: 100 μm. (**E**) Representative Western blot bands of NeuN in hippocampus. (**F**) Quantification of the NeuN protein levels in the control, KA and lactate groups (n=3 in each group). The data are presented as the means ± SDs. Significance was determined by one-way ANOVA followed by Tukey's post hoc test (**P*<0.05, ***P*<0.01).

Lactate Treatment Ameliorates Anxiety-Like Behavior and Improves Cognitive Function and Motor Balance Performance in Epileptic Mice

To assess the functional changes induced by lactate treatment, the open field test, novel object recognition test, and rotarod test were carried out to assess anxiety-like behavior, cognitive function, and motor balance performance, respectively. In the open field test (Figure 5A and B), the distance traveled and time spent in the center decreased significantly in the KA group (Figure 5C–E; ANOVA, **P* < 0.05, ****P* < 0.001). However, they were visibly increased in the lactate group, and there was no difference between the control and lactate groups (Figure 5C and D; ANOVA, **P* < 0.05, ****P* < 0.001). No significant difference was found in the total distance traveled among the three groups (Figure 5E; ANOVA). These results suggested that

https://doi.org/10.2147/JIR.S498738

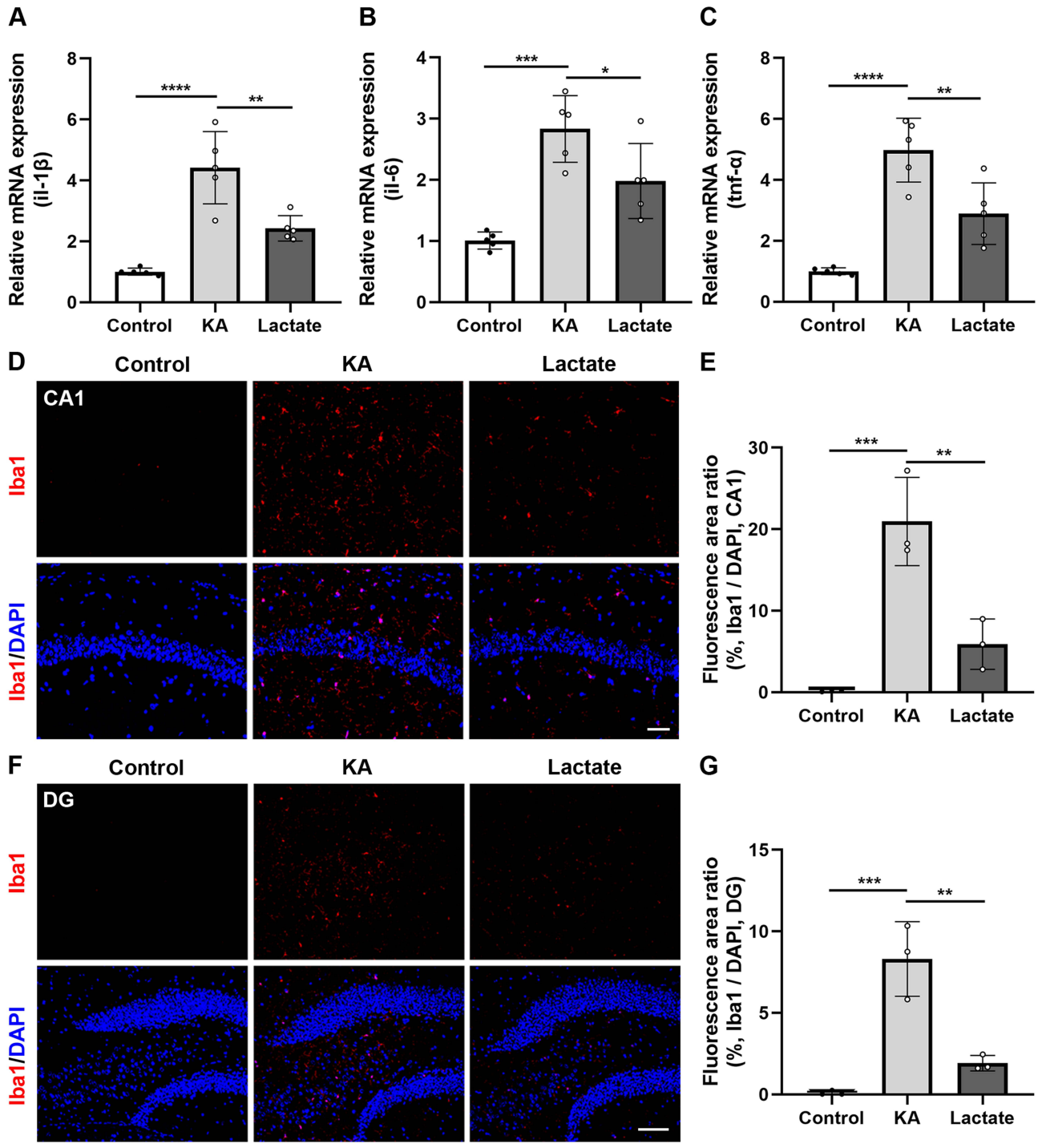

Figure 4 Microglial activation and inflammatory factor expression in the hippocampi of acute epileptic and lactate-treated mice. (**A**–**C**) The relative mRNA expression levels of the inflammatory factors *il-1β* (**A**), *il-6* (**B**) and *tnf-α* (**C**) in the hippocampus of the control, KA and lactate groups (n=5 in each group). (**D**) Images of Iba1 immunofluorescence staining in the CA1 region in the control, KA and lactate groups. Scale bar: 50 μm. (**E**) Quantification of the ratio of the Iba1/DAPI area in the CA1 region (n=3 in each group). (**F**) Images of Iba1 immunofluorescence staining in the DG region in the control, KA and lactate groups. Scale bar: 100 μm. (**G**) Quantification of the ratio of the Iba1/DAPI area in the DG region (n=3 in each group). The data are presented as the means ± SDs. Significance was determined by one-way ANOVA followed by Tukey's post hoc test (**P*<0.05, ***P*<0.01, ****P*<0.001, *****P*<0.0001).

the anxiety-like behavior of mice with acute seizures was alleviated by lactate intervention. The time spent on the rotarod and distance traveled on the rotarod were evidently increased in the lactate-treated mice compared to the KA-induced mice, suggesting that the motor coordination and balance of the mice were improved after lactate treatment (Figure 5F and G;

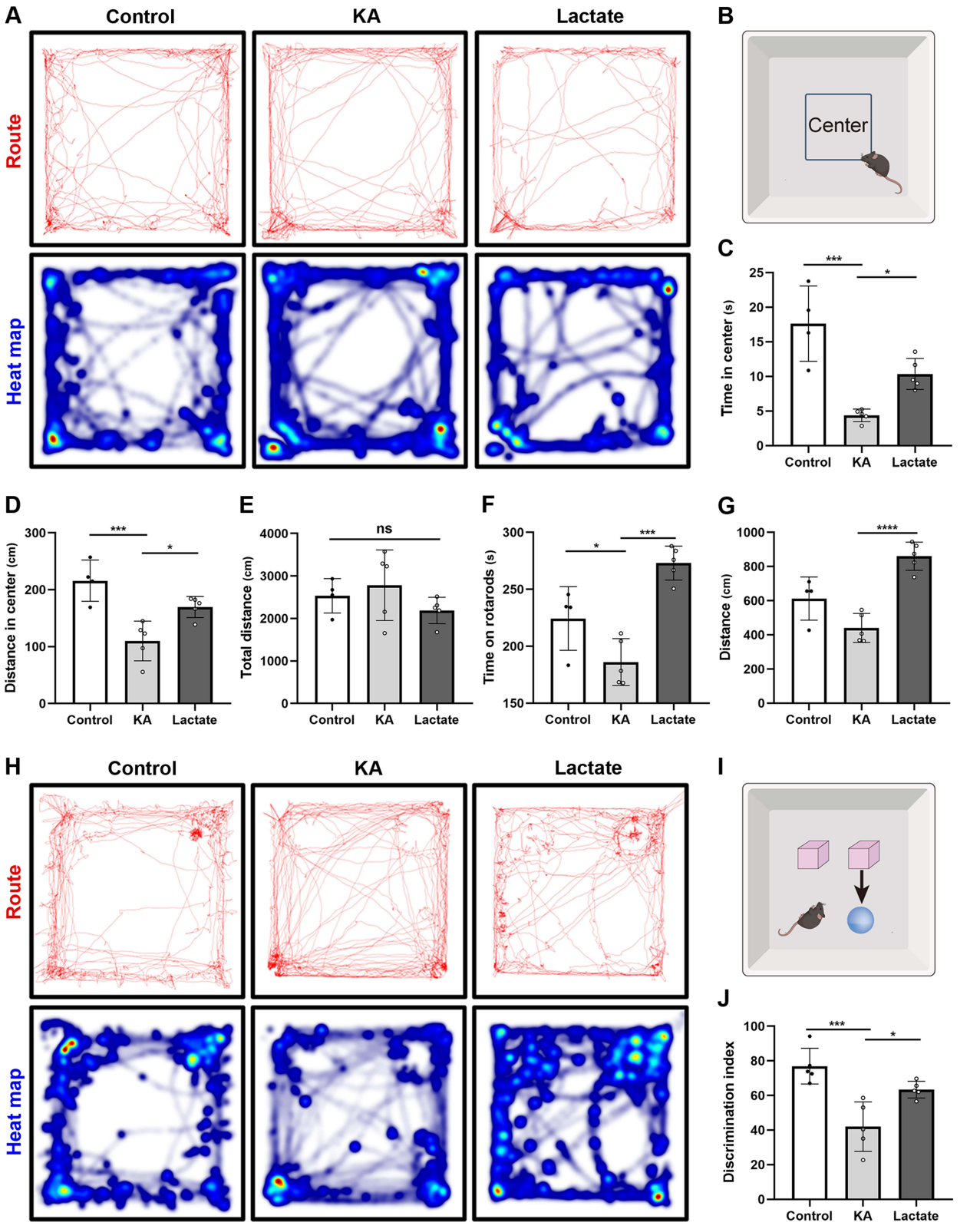

Figure 5 Behavioural tests and analysis in KA-induced acute epileptic and lactate-treated mice. (**A**) Representative routes and heat maps in the open field experiment in mice from the control (n=4), KA (n=5) and lactate (n=5) groups. (**B**) Diagram of the open field experiment. (**C**–**E**) Statistical analysis of the time spent in the centre (**C**), distance travelled in the centre (**D**) and total distance travelled (**E**) by the mice. (**F** and **G**) Time (**F**) and distance travelled (**G**) on the rotarod in mice in the control (n=4), KA (n=5) and lactate (n=5) groups. (**H**) Representative routes and heat maps in the novel object recognition test (n=5 in each group). (**I**) Diagram of the novel object recognition test. (**J**) Statistical analysis of the discrimination index. The data are presented as the means ± SDs. Significance was determined by one-way ANOVA followed by Tukey's post hoc test (ns, not significant; **P*<0.05, ****P*<0.001, *****P*<0.0001).

https://doi.org/10.2147/JIR.S498738

ANOVA, *$P < 0.05$, ***$P < 0.001$, ****$P < 0.001$). In the novel object recognition test, the time spent sniffing the novel object was decreased in the KA group and increased in the lactate group, as indicated by an increase in the discrimination index (Figure 5H–J; ANOVA, *$P < 0.05$, ***$P < 0.001$), suggesting that lactate treatment improved short-term memory. The above data demonstrate that lactate treatment effectively ameliorates anxiety-like behavior and improves motor balance performance and cognitive function in epileptic mice.

Lactate Treatment Significantly Alters Transcript Levels in Epileptic Mice

To identify alterations in gene expression following lactate treatment, five ipsilateral hippocampal tissues from each group were collected, and RNA-seq was performed 5 days after lactate treatment. The quality control metrics of the mapped reads for each RNA-seq sample are listed in Table 2. The Venn diagram in Figure 6A showed the number of genes coexpressed among the three groups and the number of genes uniquely expressed in each group. Figure 6B was the heat map of the differential gene expression profiles following KA induction and lactate treatment. A total of 920 genes were significantly differentially expressed at the transcriptome level between the control and KA groups. Among them, 528 genes were upregulated, while 392 genes were downregulated (Figure 6C). A total of 727 genes were obviously altered between the control and lactate groups. Among these genes, 368 had increased expression and 359 had decreased expression (Figure 6D). A total of 195 differentially expressed genes (DEGs) were identified between the KA and lactate groups, including 55 upregulated and 140 downregulated genes (Figure 6E). To confirm the reliability of the RNA-seq data, we further selected 8 DEGs with large fold changes, namely, fcnb, trdn, fam124b, olfr5, emilin3, lrr1, slc15a1, and gbp10, and quantified their expression levels by qRT-PCR. The expression changes, regardless of up- or downregulation, were in accordance with the RNA-seq results (Figure 6F and G). These results prove that lactate treatment leads to significant changes at the transcriptional level in KA-induced mice.

Enrichment Analysis and PPI Network Analysis Reveal That Lactate Acts Through the Chemokine Signaling Pathway to Exert Its Therapeutic Effects

GO analysis, KEGG analysis, and GSEA were carried out on the DEGs for functional annotation and pathway enrichment analysis. GO enrichment analysis includes three categories: biological process (BP), cellular component (CC), and molecular function (MF). Among the DEGs in the KA and control groups, defense response to other organisms contained in the BP category, mitochondrial membrane part in the CC category, and electron transfer activity in the MF

Table 2 Sequencing Quality Control Metrics

Sample	Clean_reads	Clean_bases	Error_rate (%)	Q20	Q30	GC_pct
Control 1	42,838,144	6.43G	0.02	97.93	94.29	49.09
Control 2	44,270,680	6.64G	0.02	97.98	94.36	49.03
Control 3	42,153,502	6.32G	0.02	97.96	94.26	49.12
Control 4	42,597,930	6.39G	0.02	98.03	94.5	51.85
Control 5	41,882,234	6.28G	0.02	98.07	94.64	51.47
KA 1	40,125,332	6.02G	0.03	96.56	91.14	49.73
KA 2	45,022,682	6.75G	0.03	96.96	92.03	49.62
KA 3	43,123,532	6.47G	0.03	97.05	92.21	49.5
KA 4	40,127,806	6.02G	0.03	96.33	90.65	49.7
KA 5	44,463,848	6.67G	0.03	96.03	90.03	49.85
Lactate 1	45,692,370	6.85G	0.03	97.13	92.3	49.76
Lactate 2	42,391,982	6.36G	0.03	96.93	91.93	49.8
Lactate 3	42,443,408	6.37G	0.03	96.57	91.18	49.99
Lactate 4	43,391,778	6.51G	0.03	96.95	92	50.02
Lactate 5	44,882,328	6.73G	0.03	96.94	92	49.48

Notes: Q20: the Phred values greater than 20 bases as a percentage of the total bases; Q30: the Phred values greater than 30 bases as a percentage of the total bases; GC_pct: the number of G and C bases as a percentage of the total bases in clean reads.

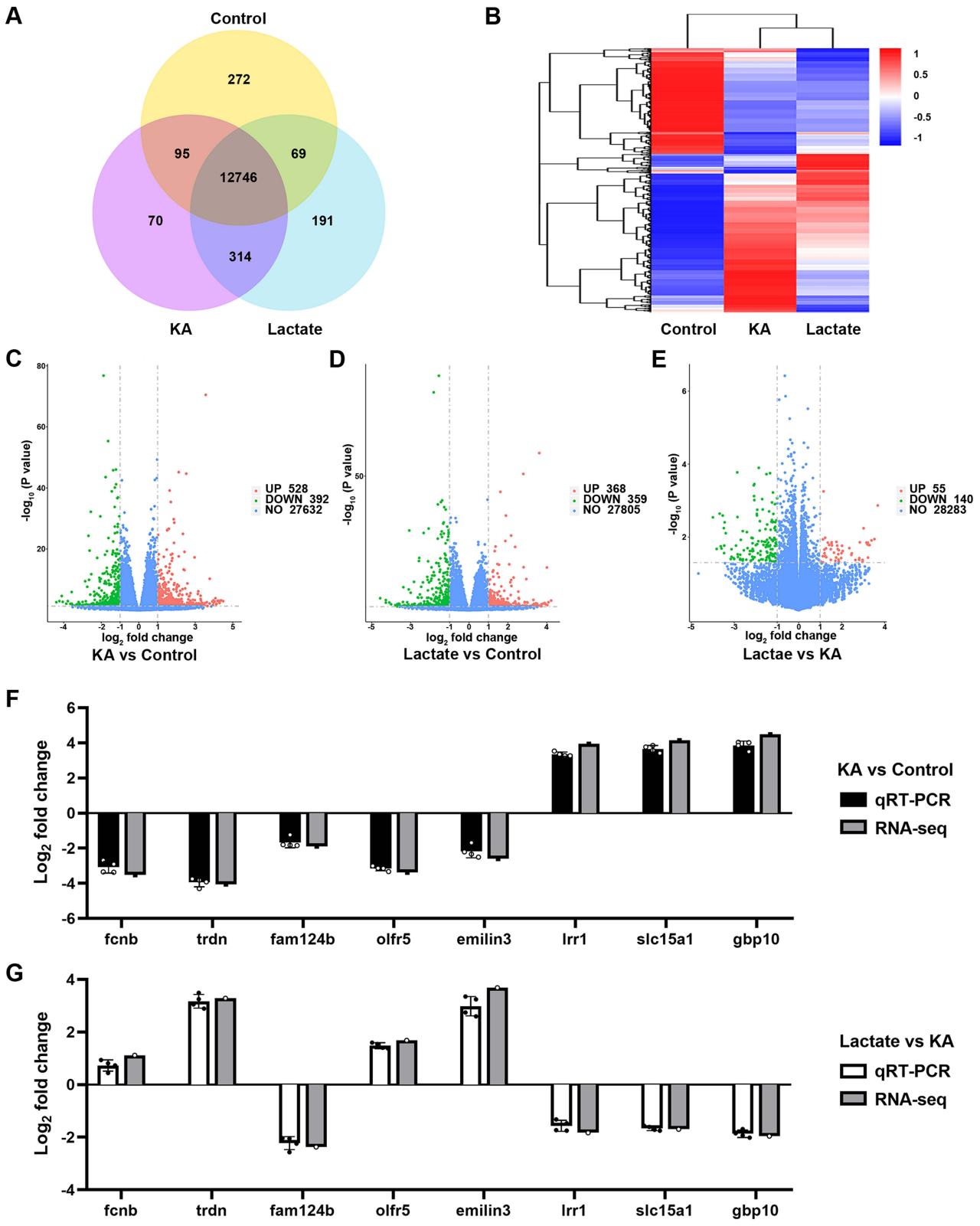

Figure 6 Differential hippocampal gene expression profiles detected by RNA-seq. (**A**) Venn diagram of coexpressed genes in the control, KA and lactate groups (n=5 in each group). (**B**) Cluster analysis of DEGs among the three groups. (**C**–**E**) Volcano plot of DEGs between the KA group and control group (**C**), between the lactate group and control group (**D**), and between the lactate group and KA group (**E**). (**F** and **G**) The expression of eight selected genes between the KA and control groups (**F**) and between the lactate and KA groups (**G**) according to qRT–PCR (n=4 in each group) and RNA sequencing (represented as log_2-fold change values).

https://doi.org/10.2147/JIR.S498738

category were enriched in most of the DEGs (Figure 7A). Among the DEGs in the lactate and KA groups, defense response to other organisms in the BP category, symbiont-containing vacuole in the CC category, and G-protein coupled receptor binding in the MF category were enriched in most of the DEGs (Figure 7B). KEGG analysis revealed that KA induction mainly regulated genes involved in oxidative phosphorylation (Figure 7C), while lactate treatment strongly regulated genes involved in the chemokine signaling pathway (Figure 7D). The expression of chemokines, including ccl5, cxcl5, cxcl9, cxcl10, cxcl13, and ccl27b, increased after KA induction but decreased after lactate treatment according to the RNA-seq results (Figure 7E). GSEA revealed differences in the expression of genes involved in the chemokine signaling pathway among the three groups by a different enrichment method, with increased expression in the KA group and decreased expression in the control and lactate groups (Figure 7F and G). We then analyzed the predicted protein interactions of DEGs between the KA and lactate groups, and the results showed that the key regulatory proteins of these genes included cxcl10, zbp1, and irf7 (Figure 7H). Therefore, lactate treatment alleviates KA-induced neuronal damage and neuroinflammation through the chemokine signaling pathway.

Multiple Inflammation-Related Signaling Pathways are Involved in the Modulation of Cognitive Function

WGCNA was performed to identify genes that were associated with cognitive impairment. The soft threshold used in this analysis was 3, with a scale-free fit value greater than 0.8 (Figure 8A and B). A cluster tree was constructed according to the correlation between gene expression levels (Figure 8C), and the y-axis represented the distance between genes. The greater the distance was, the lower the similarity. Nine different gene modules were identified (red, pink, green, black, yellow, turquoise, blue, brown and grey). Unassigned genes are displayed in the grey module, and the expression patterns of genes clustered within the other 8 modules were shown as heat maps and bar graphs in Supplemental Figures 2 and 3. The correlations between module eigengenes (MEs) were calculated and presented in a dendrogram and heat map in Figure 8D. Correlations between each ME and sample traits (inflammatory factors il-1β, il-6, tnf-α and discrimination index) were calculated, and the MEturquoise module correlated best with the discrimination index among all modules, implying that genes in the MEturquoise module were most important for cognitive changes in mice (Figure 8E). Additionally, the MEturquoise module also correlated well with inflammatory factors, suggesting that genes in the MEturquoise module were able to reflect both cognitive and inflammatory states. Subsequently, genes in the MEturquoise module were subjected to GO and KEGG enrichment analyses. The most enriched GO annotation terms were ribonucleoprotein complex biogenesis, organelle inner membrane, and transcription cofactor activity (Figure 8F). The most enriched KEGG pathways included the mTOR, FoxO, Ras, and MAPK pathways, all of which were involved in inflammation, as well as significant enrichment in the chemokine signaling pathway (Figure 8G). Once again, from a different perspective, lactate attenuates neuroinflammation and cognitive impairment by modulating chemokines. Furthermore, these results indicate that a variety of inflammatory pathways are involved in the regulation of cognitive status.

Discussion

HCAR1 was shown to be expressed in the brain tissues of epilepsy patients following surgical resection as well as in those of epileptic mice. Moreover, neuronal activity can be reduced after HCAR1 activation with exogenous agonists.[19] Using the whole-cell patch-clamp technique, researchers found that the application of lactate and exogenous agonists could reduce the excitatory postsynaptic current frequency and spontaneous calcium spike activity of primary cortical neurons in mice.[20] Jorwal et al established an in vitro epilepsy model in acute rat hippocampal slices and found that lactate activated the GIRK channel via HCAR1 to decrease epileptiform activity in neurons.[21] However, the above studies were carried out in acute brain slice models, and the role of lactate in epilepsy still needs to be further explored. Both in vitro and in vivo experiments were conducted in our study to clarify the effects of lactate on seizure-induced neuronal injury and the underlying mechanisms involved.

The mouse hippocampal-derived HT22 cell line has been widely used to construct in vitro models of neurological disorders.[22,23] Moreover, glutamate stimulation leads to pathological changes in Alzheimer's disease, Parkinson's

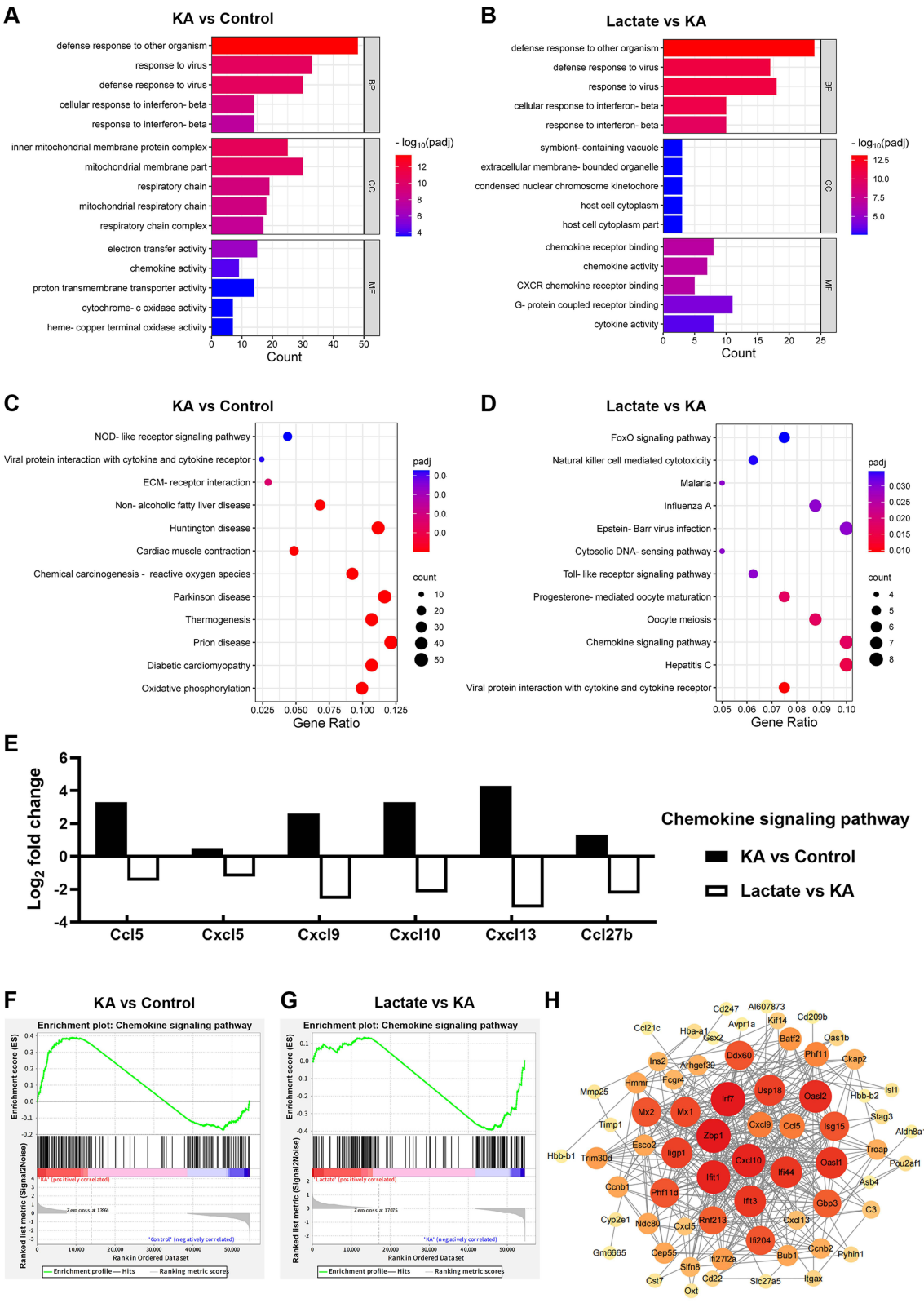

Figure 7 Gene enrichment analysis and PPI network analysis of differentially expressed genes. (**A**) GO categorization of DEGs between the KA group and the control group. GO terms: biological process (BP), cellular component (CC), molecular function (MF). (**B**) GO categorization of DEGs between the lactate group and KA group. (**C**) KEGG assignment of DEGs between the KA group and control group. (**D**) KEGG assignment of DEGs between the lactate group and KA group. (**E**) Log_2 fold change values of a panel of chemokines among the control, KA and lactate groups determined by RNA sequencing. (**F**) GSEA of the enrichment plot of chemokine signaling pathway between the KA group and the control group. (**G**) GSEA plot of chemokine signaling pathway enrichment between the lactate group and the KA group. (**H**) PPI network analysis of DEGs.

https://doi.org/10.2147/JIR.S498738

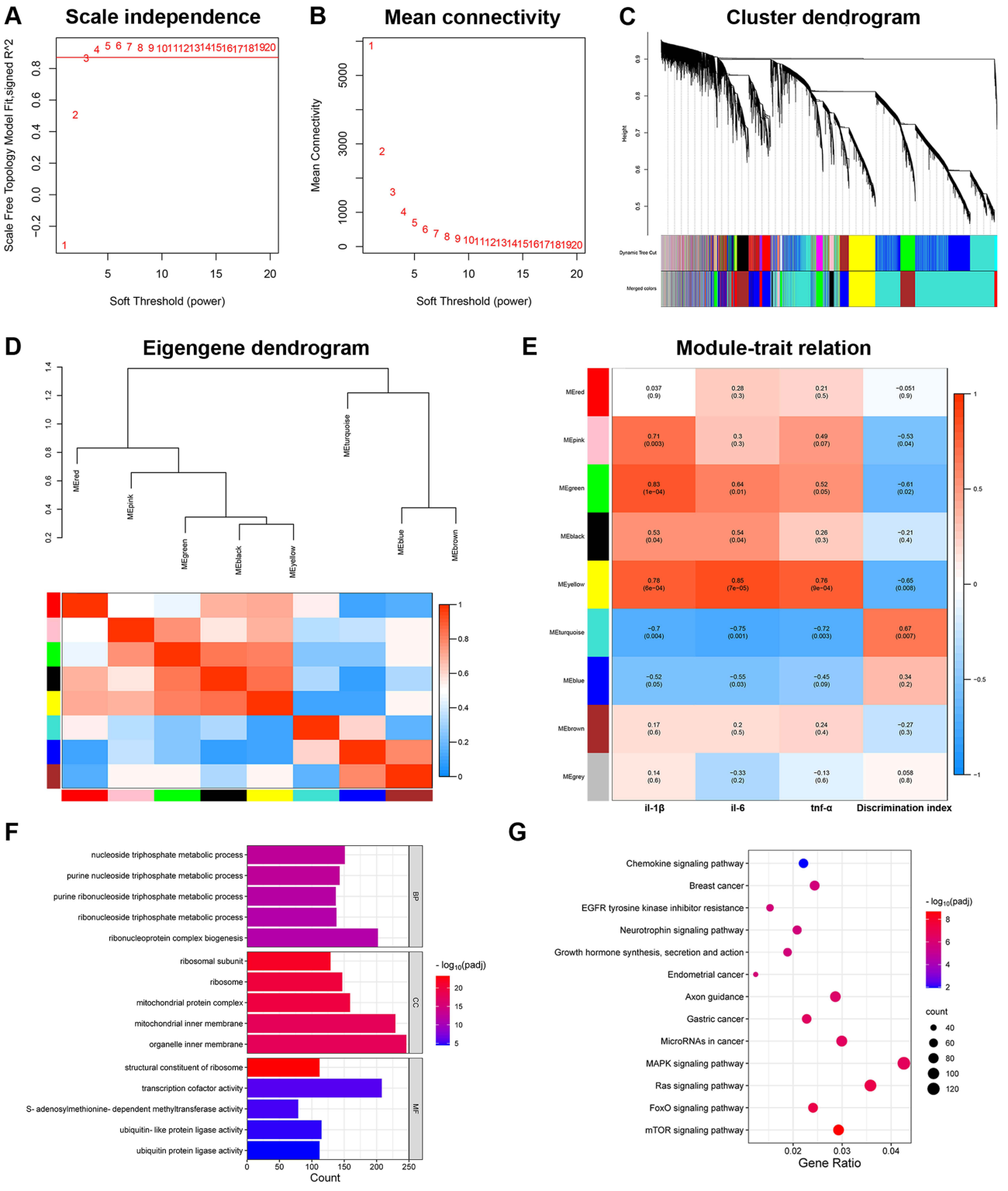

Figure 8 Identification of the most relevant module for cognitive performance using WGCNA and its gene enrichment analysis. (**A**) Scale-free topology fit index analysis. (**B**) The mean connectivity analysis. (**C**) Module clustering tree after merging. (**D**) Heat map showing the correlations among all of the modules. (**E**) Heat map showing the correlations between each gene module with sample traits. (**F**) Enriched GO terms in the turquoise module genes. (**G**) KEGG annotation of the genes in the turquoise module.

disease, and epilepsy.[24–26] In this study, we established an excitotoxic injury model by stimulating HT22 cells with glutamate, which was verified by the high expression of *c-fos*, a marker of neuronal activity. Apoptosis and the release of inflammatory factors mimicked the pathological changes that occur under epileptic conditions.[27,28] In contrast, as lactate treatment successfully increased the expression of *hcar1* in HT22 cells, these pathological changes were abrogated. Vesicular glutamate transporters (VGLUTs), which can load and release glutamate into and from vesicles, are specific markers for glutamatergic neurons, and three isoforms have been identified, including VGLUT1, VGLUT2 and VGLUT3.[29,30] The content of excitatory synaptic components represented by VGLUT1 increased considerably during epileptogenesis, which has been observed in various subregions of the hippocampus.[31] In our in vitro model, VGLUT1 was notably elevated under glutamate stimulation, indicating a significant increase in glutamate transport in HT22 cells, whereas the expression of VGLUT1 was markedly reduced in lactate-treated cells. Therefore, the lactate/HCAR1 system attenuated apoptosis, inflammation, and excitotoxic injury by inhibiting glutamate uptake by neuronal cells.

The KA-induced epilepsy model is commonly used to study this disease. We observed significant neuronal loss, microglial activation, and inflammatory factor upregulation after intraperitoneal injection of KA.[32,33] However, after lactate treatment, more neurons survived, while fewer microglia were activated in the hippocampus. Moreover, the release of inflammatory factors was suppressed. Behavioral tests revealed that lactate treatment alleviated anxiety-like behaviors and cognitive impairment caused by seizures. Additionally, lactate has been used in the experimental treatment of acute ischemic stroke and neonatal hypoxic-ischemic encephalopathy, and our results further support the hypothesis that lactate can be used as a neuroprotective agent in epilepsy.[34–36] Notably, glycogen-derived lactate is beneficial for memory consolidation, and lactate can promote neurogenesis in the brain.[37,38] Whether lactate plays a role in improving cognitive function by alleviating pathological damage or by consolidating memory and neurogenesis itself needs to be further explored.

RNA-seq is a genomic method for the detection and quantitative analysis of RNA molecules in biological samples and has been widely used to visualize the transcriptome of the brain.[39] The enrichment results revealed that the chemokine signaling pathway played an important role in the effects of lactate treatment. Chemokine signaling is involved in a variety of biological processes, including cell polarization, migration, and inflammatory responses. Its regulation is highly important in diseases such as ischemic brain injury, neurodegenerative diseases, and cancer.[40–43] Several studies on epilepsy have reported the antiepileptic, anti-inflammatory, and neuroprotective effects of antagonists of various members in the chemokine signaling pathway.[44–46] It was reported that CXCL10 was upregulated in the serum of epileptic patients and the stimulation of recombinant CXCL10 increased the susceptibility to epilepsy in mice, demonstrating the important role of CXCL10 in epilepsy.[47] Consistent with this finding, our results of PPI network analysis identified CXCL10 as the hub gene for lactate treatment. We determined that lactate downregulated the expression of a series of chemokines represented by CXCL10, thereby improving the neuropathological changes and neurological and neurobehavioural comorbidities induced by KA injection.

Cognitive impairment is one of the main complications of epilepsy and gradually worsens as epilepsy progresses, further exacerbating the burden on patients.[48,49] Brain inflammation is related to epilepsy and seizure-induced cognitive impairment, and studies have shown that reducing inflammation alleviates the cognitive impairment caused by epilepsy in animal models.[50,51] The results of our WGCNA also support this view, and we found that genes in the turquoise module, which was most strongly associated with cognitive status, were remarkably enriched in inflammatory pathways, such as the mTOR, FoxO, Ras, MAPK, neutrophin, and chemokine signaling pathways, identifying a close link between inflammation and cognitive impairment caused by epilepsy.[52–54] It is evident that multiple inflammatory pathways function concurrently in the process of cognitive impairment. Using mTOR inhibitors, the neurological signs and cognitive impairment of tuberous sclerosis were improved.[55] Also, it was found that Akt-FoxO3a signaling was associated with seizure-induced neuronal death, suggesting that the inhibition of different inflammatory pathways might alleviate seizures and cognitive deficits.[56] This finding suggests that maintaining the cognitive function in mice is such a complex and complete process involving multiple signaling pathways. Treatments targeting multiple inflammation-related pathways may have more ideal effects and are worthy of further research in the future.

Conclusion

Lactate intervention mitigates neuronal damage, reduces excitatory neurotransmitter uptake, and ameliorates the inflammatory microenvironment in kainic acid-induced epilepsy mice. CXCL10 is the hub site for the neuroprotective effects of

lactate. mTOR, FoxO, Ras, MAPK, neutrophin, and chemokine are multiple inflammation-related pathways involved in cognitive impairment after epilepsy, and targeting multiple inflammation-related pathways is a promising strategy for improving the prognosis of epilepsy.

Abbreviations

BP, biological process; CA, cornu ammonis; CC, cellular component; DAPI, 4',6-diamidino-2-phenylindole; DEGs, differentially expressed genes; DG, dentate gyrus; GO, gene ontology; HCAR, hydroxy-carboxylic acid receptor; KA, kainic acid; KEGG, Kyoto encyclopedia of genes and genomes; MEs, module eigengenes; MF, molecular function; PPI, protein–protein interaction; qRT–PCR, quantitative real-time polymerase chain reaction; RNA-seq, RNA sequencing; SE, status epilepticus; VGLUT1, vesicular glutamate transporter 1; WGCNA, weighted gene co-expression network analysis.

Data Sharing Statement

All data generated or analyzed during this study are included in this published article and Supplemental Data.

Ethics Approval Statement

All animal experimental protocols were approved by the Laboratory Animal Welfare and Ethics Committee of Xuanwu Hospital, Capital Medical University (permission number: XW20220906-1).

Acknowledgments

This work was supported by Beijing Natural Science Foundation (No. 7242066); the National Natural Science Foundation of China (No. 82030037), Foundation of Human Brain Banking in Beijing Geriatric Medical Research About Pathological Mechanism Study of Neurological Diseases, Beijing Municipal Health Commission (No. 11000024T000002829630); and the Open Project of Institute of Optometry and Vision Science in Nankai University (No. NKSGY202302-2024430HJ0323).

Disclosure

The authors report no conflicts of interest in this work.

References

1. Thijs RD, Surges R, O'Brien TJ, Sander JW. Epilepsy in adults. *Lancet*. 2019;393(10172):689–701. doi:10.1016/S0140-6736(18)32596-0
2. Tian N, Boring M, Kobau R, Zack MM, Croft JB. Active Epilepsy and Seizure Control in Adults - United States, 2013 and 2015. *MMWR Morb Mortal Wkly Rep*. 2018;67(15):437–442. doi:10.15585/mmwr.mm6715a1
3. Chen Y, Nagib MM, Yasmen N, et al. Neuroinflammatory mediators in acquired epilepsy: an update. *Inflamm Res*. 2023;72(4):683–701. doi:10.1007/s00011-023-01700-8
4. Pracucci E, Pillai V, Lamers D, Parra R, Landi S. Neuroinflammation: a Signature or a Cause of Epilepsy? *Int J mol Sci*. 2021;22(13):6981. doi:10.3390/ijms22136981
5. Magistretti PJ, Allaman I. Lactate in the brain: from metabolic end-product to signalling molecule. *Nat Rev Neurosci*. 2018;19(4):235–249. doi:10.1038/nrn.2018.19
6. Wallenius K, Thalen P, Bjorkman JA, et al. Involvement of the metabolic sensor GPR81 in cardiovascular control. *JCI Insight*. 2017;2(19):e92564. doi:10.1172/jci.insight.92564
7. Ranganathan P, Shanmugam A, Swafford D, et al. GPR81, a Cell-Surface Receptor for Lactate, Regulates Intestinal Homeostasis and Protects Mice from Experimental Colitis. *J Immunol*. 2018;200(5):1781–1789. doi:10.4049/jimmunol.1700604
8. Brown TP, Bhattacharjee P, Ramachandran S, et al. The lactate receptor GPR81 promotes breast cancer growth via a paracrine mechanism involving antigen-presenting cells in the tumor microenvironment. *Oncogene*. 2020;39(16):3292–3304. doi:10.1038/s41388-020-1216-5
9. Vardjan N, Chowdhury HH, Horvat A, et al. Enhancement of Astroglial Aerobic Glycolysis by Extracellular Lactate-Mediated Increase in cAMP. *Front Mol Neurosci*. 2018;11:148. doi:10.3389/fnmol.2018.00148
10. Boitsova EB, Morgun AV, Osipova ED, et al. The inhibitory effect of LPS on the expression of GPR81 lactate receptor in blood-brain barrier model in vitro. *J Neuroinflammation*. 2018;15(1):196. doi:10.1186/s12974-018-1233-2
11. Lev-Vachnish Y, Cadury S, Rotter-Maskowitz A, et al. L-Lactate Promotes Adult Hippocampal Neurogenesis. *Front Neurosci*. 2019;13:403. doi:10.3389/fnins.2019.00403
12. Jourdain P, Allaman I, Rothenfusser K, Fiumelli H, Marquet P, Magistretti PJ. L-Lactate protects neurons against excitotoxicity: implication of an ATP-mediated signaling cascade. *Sci Rep*. 2016;6:21250.

13. Orsini A, Diquigiovanni C, Bonora E. Omics Technologies Improving Breast Cancer Research and Diagnostics. *Int J mol Sci*. 2023;24(16):12690. doi:10.3390/ijms241612690
14. Banerjee S, Prabhu BN, PS R. Omics technologies in personalized combination therapy for cardiovascular diseases: challenges and opportunities. *Per Med*. 2021;18(6):595–611. doi:10.2217/pme-2021-0087
15. Du Y, Li R, Fu D, et al. Multi-omics technologies and molecular biomarkers in brain tumor-related epilepsy. *CNS Neurosci Ther*. 2024;30(4): e14717. doi:10.1111/cns.14717
16. Du Y, Li Z, Liu Z, et al. Nonrandom occurrence of multiple de novo coding variants in a proband indicates the existence of an oligogenic model in autism. *Genet Med*. 2020;22(1):170–180. doi:10.1038/s41436-019-0610-2
17. Jin J, Li K, Du Y, Gao F, Wang Z, Li W. Multi-omics study identifies that PICK1 deficiency causes male infertility by inhibiting vesicle trafficking in Sertoli cells. *Reprod Biol Endocrinol*. 2023;21(1):114. doi:10.1186/s12958-023-01163-w
18. Racine RJ. Modification of seizure activity by electrical stimulation. II. Motor seizure. *Electroencephalogr Clin Neurophysiol*. 1972;32(3):281–294. doi:10.1016/0013-4694(72)90177-0
19. Briquet M, Rocher AB, Alessandri M, et al. Activation of lactate receptor HCAR1 down-modulates neuronal activity in rodent and human brain tissue. *J Cereb Blood Flow Metab*. 2022;42(9):1650–1665. doi:10.1177/0271678X221080324
20. de Castro Abrantes H, Briquet M, Schmuziger C, et al. The Lactate Receptor HCAR1 Modulates Neuronal Network Activity through the Activation of G(alpha) and G(betagamma) Subunits. *J Neurosci*. 2019;39(23):4422–4433. doi:10.1523/JNEUROSCI.2092-18.2019
21. Jorwal P, Sikdar SK. Lactate reduces epileptiform activity through HCA1 and GIRK channel activation in rat subicular neurons in an in vitro model. *Epilepsia*. 2019;60(12):2370–2385. doi:10.1111/epi.16389
22. Chang X, Niu S, Shang M, et al. ROS-Drp1-mediated mitochondria fission contributes to hippocampal HT22 cell apoptosis induced by silver nanoparticles. *Redox Biol*. 2023;63:102739. doi:10.1016/j.redox.2023.102739
23. Prasansuklab A, Sukjamnong S, Theerasri A, Hu VW, Sarachana T, Tencomnao T. Transcriptomic analysis of glutamate-induced HT22 neurotoxicity as a model for screening anti-Alzheimer's drugs. *Sci Rep*. 2023;13(1):7225. doi:10.1038/s41598-023-34183-y
24. Revett TJ, Baker GB, Jhamandas J, Kar S. Glutamate system, amyloid ss peptides and tau protein: functional interrelationships and relevance to Alzheimer disease pathology. *J Psychiatry Neurosci*. 2013;38(1):6–23. doi:10.1503/jpn.110190
25. Lange KW, Kornhuber J, Riederer P. Dopamine/glutamate interactions in Parkinson's disease. *Neurosci Biobehav Rev*. 1997;21(4):393–400. doi:10.1016/S0149-7634(96)00043-7
26. Green JL, Dos Santos WF, Fontana ACK. Role of glutamate excitotoxicity and glutamate transporter EAAT2 in epilepsy: opportunities for novel therapeutics development. *Biochem Pharmacol*. 2021;193:114786. doi:10.1016/j.bcp.2021.114786
27. Xie R, Zhao W, Lowe S, et al. Quercetin alleviates kainic acid-induced seizure by inhibiting the Nrf2-mediated ferroptosis pathway. *Free Radic Biol Med*. 2022;191:212–226. doi:10.1016/j.freeradbiomed.2022.09.001
28. Wang Y, Li C, Xiong Z, et al. Up-and-coming anti-epileptic effect of aloesone in Aloe vera: evidenced by integrating network pharmacological analysis, in vitro, and in vivo models. *Front Pharmacol*. 2022;13:962223. doi:10.3389/fphar.2022.962223
29. Neale SA, Copeland CS, Salt TE. Effect of VGLUT inhibitors on glutamatergic synaptic transmission in the rodent hippocampus and prefrontal cortex. *Neurochem Int*. 2014;73:159–165. doi:10.1016/j.neuint.2013.10.001
30. El Mestikawy S, Wallen-Mackenzie A, Fortin GM, Descarries L, Trudeau LE. From glutamate co-release to vesicular synergy: vesicular glutamate transporters. *Nat Rev Neurosci*. 2011;12(4):204–216. doi:10.1038/nrn2969
31. Fan J, Dong X, Tang Y, et al. Preferential pruning of inhibitory synapses by microglia contributes to alteration of the balance between excitatory and inhibitory synapses in the hippocampus in temporal lobe epilepsy. *CNS Neurosci Ther*. 2023;29(10):2884–2900. doi:10.1111/cns.14224
32. Zhang X, Liang P, Zhang Y, et al. Blockade of Kv1.3 Potassium Channel Inhibits Microglia-Mediated Neuroinflammation in Epilepsy. *Int J mol Sci*. 2022;23(23):14693. doi:10.3390/ijms232314693
33. Chang A, Chang Y, Wang SJ. Rutin prevents seizures in kainic acid-treated rats: evidence of glutamate levels, inflammation and neuronal loss modulation. *Food Funct*. 2022;13(20):10401–10414. doi:10.1039/D2FO01490D
34. Geiseler SJ, Hadzic A, Lambertus M, et al. L-Lactate Treatment at 24 h and 48 h after Acute Experimental Stroke Is Neuroprotective via Activation of the L-Lactate Receptor HCA(1). *Int J mol Sci*. 2024;25(2):1232. doi:10.3390/ijms25021232
35. Roumes H, Dumont U, Sanchez S, et al. Neuroprotective role of lactate in rat neonatal hypoxia-ischemia. *J Cereb Blood Flow Metab*. 2021;41 (2):342–358. doi:10.1177/0271678X20908355
36. Tassinari ID, Andrade MKG, da Rosa LA, et al. Lactate Administration Reduces Brain Injury and Ameliorates Behavioral Outcomes Following Neonatal Hypoxia-Ischemia. *Neuroscience*. 2020;448:191–205. doi:10.1016/j.neuroscience.2020.09.006
37. Vezzoli E, Cali C, De Roo M, et al. Ultrastructural Evidence for a Role of Astrocytes and Glycogen-Derived Lactate in Learning-Dependent Synaptic Stabilization. *Cereb Cortex*. 2020;30(4):2114–2127. doi:10.1093/cercor/bhz226
38. Lambertus M, Overberg LT, Andersson KA, et al. L-lactate induces neurogenesis in the mouse ventricular-subventricular zone via the lactate receptor HCA(1). *Acta Physiol*. 2021;231(3):e13587. doi:10.1111/apha.13587
39. Haque A, Engel J, Teichmann SA, Lonnberg T. A practical guide to single-cell RNA-sequencing for biomedical research and clinical applications. *Genome Med*. 2017;9(1):75. doi:10.1186/s13073-017-0467-4
40. Mellado M, Rodriguez-Frade JM, Manes S, Martinez AC. Chemokine signaling and functional responses: the role of receptor dimerization and TK pathway activation. *Annu Rev Immunol*. 2001;19(1):397–421. doi:10.1146/annurev.immunol.19.1.397
41. Zhang XQ, Wang XY, Dong BC, et al. C-X-C chemokine receptor type 7 antibody enhances neural plasticity after ischemic stroke. *Neural Regen Res*. 2023;18(9):1976–1982. doi:10.4103/1673-5374.363835
42. Wei L, Yang X, Wang J, et al. H3K18 lactylation of senescent microglia potentiates brain aging and Alzheimer's disease through the NFkappaB signaling pathway. *J Neuroinflammation*. 2023;20(1):208. doi:10.1186/s12974-023-02879-7
43. Teicher BA, Fricker SP. CXCL12 (SDF-1)/CXCR4 pathway in cancer. *Clin Cancer Res*. 2010;16(11):2927–2931. doi:10.1158/1078-0432.CCR-09-2329
44. Cerri C, Genovesi S, Allegra M, et al. The Chemokine CCL2 Mediates the Seizure-enhancing Effects of Systemic Inflammation. *J Neurosci*. 2016;36(13):3777–3788. doi:10.1523/JNEUROSCI.0451-15.2016
45. Xu T, Yu X, Deng J, et al. CXCR7 regulates epileptic seizures by controlling the synaptic activity of hippocampal granule cells. *Cell Death Dis*. 2019;10(11):825. doi:10.1038/s41419-019-2052-9

46. Zhang Z, Li Y, Jiang S, Shi FD, Shi K, Jin WN. Targeting CCL5 signaling attenuates neuroinflammation after seizure. *CNS Neurosci Ther*. 2023;29(1):317–330. doi:10.1111/cns.14006
47. Liang P, Zhang X, Zhang Y, et al. Neurotoxic A1 astrocytes promote neuronal ferroptosis via CXCL10/CXCR3 axis in epilepsy. *Free Radic Biol Med*. 2023;195:329–342. doi:10.1016/j.freeradbiomed.2023.01.002
48. Operto FF, Pastorino GMG, Viggiano A, et al. Epilepsy and Cognitive Impairment in Childhood and Adolescence: a Mini-Review. *Curr Neuropharmacol*. 2023;21(8):1646–1665. doi:10.2174/1570159X20666220706102708
49. Sen A, Jette N, Husain M, Sander JW. Epilepsy in older people. *Lancet*. 2020;395(10225):735–748. doi:10.1016/S0140-6736(19)33064-8
50. Dong X, Fan J, Lin D, et al. Captopril alleviates epilepsy and cognitive impairment by attenuation of C3-mediated inflammation and synaptic phagocytosis. *J Neuroinflammation*. 2022;19(1):226. doi:10.1186/s12974-022-02587-8
51. Hoda U, Jain S, Samim M, Jain GK, Agarwal NB. Embelin ameliorates cognitive dysfunction and progression of kindling in pentylenetetrazol-induced kindling in mice by attenuating brain inflammation. *Epilepsy Behav*. 2021;116:107788. doi:10.1016/j.yebeh.2021.107788
52. Ravizza T, Scheper M, Di Sapia R, Gorter J, Aronica E, Vezzani A. mTOR and neuroinflammation in epilepsy: implications for disease progression and treatment. *Nat Rev Neurosci*. 2024;25(5):334–350. doi:10.1038/s41583-024-00805-1
53. Lee JW, Nam H, Kim LE, et al. TLR4 (toll-like receptor 4) activation suppresses autophagy through inhibition of FOXO3 and impairs phagocytic capacity of microglia. *Autophagy*. 2019;15(5):753–770. doi:10.1080/15548627.2018.1556946
54. Zhang B, Zeng M, Wang Y, et al. Oleic acid alleviates LPS-induced acute kidney injury by restraining inflammation and oxidative stress via the Ras/MAPKs/PPAR-gamma signaling pathway. *Phytomedicine*. 2022;94:153818. doi:10.1016/j.phymed.2021.153818
55. Ehninger D, de Vries PJ, Silva AJ. From mTOR to cognition: molecular and cellular mechanisms of cognitive impairments in tuberous sclerosis. *J Intellect Disabil Res*. 2009;53(10):838–851. doi:10.1111/j.1365-2788.2009.01208.x
56. Kim YS, Choi MY, Lee DH, et al. Decreased interaction between FoxO3a and Akt correlates with seizure-induced neuronal death. *Epilepsy Res*. 2014;108(3):367–378. doi:10.1016/j.eplepsyres.2014.01.003